

ENACT: Entropy-based Clustering of Attention Input for Improving the Computational Performance of Object Detection Transformers

Giorgos Savathrakis¹ Antonis Argyros^{1,2}

¹ Institute of Computer Science, FORTH ² Computer Science Department, University of Crete
 {gsav, argyros}@ics.forth.gr

Abstract

Transformers demonstrate competitive performance in terms of precision on the problem of vision-based object detection. However, they require considerable computational resources due to the quadratic size of the attention weights. In this work, we propose to cluster the transformer input on the basis of its entropy. The reason for this is that the self-information of each pixel (whose sum is the entropy), is likely to be similar among pixels corresponding to the same objects. Clustering reduces the size of data given as input to the transformer and therefore reduces training time and GPU memory usage, while at the same time preserves meaningful information to be passed through the remaining parts of the network. The proposed process is organized in a module called ENACT, that can be plugged-in any transformer architecture that consists of a multi-head self-attention computation in its encoder. We ran extensive experiments using the COCO object detection dataset, and three detection transformers. The obtained results demonstrate that in all tested cases, there is consistent reduction in the required computational resources, while the precision of the detection task is only slightly reduced. The code of the ENACT module will become available at <https://github.com/GSavathrakis/ENACT>.

1. Introduction

In the period following the emergence of Deep Learning approaches to tackle computer vision problems, there has been extensive research on the problem of vision-based object detection. Several such detectors have been proposed over the years, with varying architectures. The most prevalent architecture categories of modern object detectors are single-stage and two-stage detectors, with several examples for both types. Single-stage object detectors (e.g., [15, 18, 23]), consist of a Convolutional Neural Network (CNN) which serves as a backbone, and a detection head which simultaneously predicts an objectness

score within predetermined regions, as well as the class and bounding box coordinates of the candidate object. Two-stage object detectors on the other hand (e.g., [11, 24]) share the convolutional backbone, but instead of implementing a detection head which simultaneously predicts class and bounding boxes in predetermined regions, they first learn the possible object regions, and then they classify and refine the boxes of the objects. In general, single-stage detectors are faster, and two-stage detectors are more accurate.

1.1. Transformer-based object detectors

The detector types described previously have a number of drawbacks, some of which are the significant computational complexity, or the need for a number of manually crafted components like NMS suppression or anchor generation. An idea that aimed to resolve this issue, was the development of object detectors with a transformer-like structure (e.g., [4, 35]). The input images are passed through a CNN backbone, and the resulting feature maps are supplemented with positional encodings, which provide spatial information to the network. The rest of the network follows an encoder-decoder architecture as proposed by Vaswani *et al.* [26]. Specifically, the encoder input consists of Queries, Keys and Values, all obtained from the feature map computed by the convolutional backbone. The decoder input is a set of object queries that are supplemented with learned embeddings. In the decoder part, there are two attention layers, the first being a self-attention layer where the Queries and the Keys originate from the object queries, and the second is a cross-attention layer where the Queries are the output of the first decoder attention layer and the Keys are obtained from the encoder’s output. The attention layers, however, have a disadvantage in terms of training time and required space due to their quadratic complexity $\mathcal{O}(N^2)$. This is one of the main limitations of this transformer architecture. Ideas aiming at solving this problem focused on either the restriction of the number of pixels each pixel should focus on [35], or on the clustering of pixels depending on the similarity of their features (e.g., [27, 32, 34]).

1.2. Information-based clustering

The majority of the mentioned works that implemented clustering in the attention input used the Euclidean distance of the feature vectors as the metric upon which the clustering is to be conducted. This is a sensible selection, since similar feature vectors are very likely to be in the same category. However, this strategy has two main drawbacks. First, it is very slow, since the time complexity of such a computation is $\mathcal{O}(N \cdot K \cdot d)$, where N is the number of reference points, K is the total number of pixels, and d is the dimension of the feature vector. Second, it depends on a prior knowledge regarding the data domain, in order to determine important hyperparameters (e.g., number of clusters).

To overcome these problems, we propose a different metric upon which feature similarity is to be calculated, and instead of the Euclidean distance we use the Shannon entropy of the Keys' pixels as the clustering criterion. The intuition behind this choice is that pixels that yield similar information (i.e., the quantity inside the entropy sum) will most likely correspond to a region including an object of a specific category, when also in close pixel-wise proximity. Furthermore, entropy has the additive property, meaning that the sum of the pixels' self-information is the information of the sum. This is a very convenient property for our work, because we want the clustering method to merge pixels, while retaining their information in an optimal manner.

Works that made use of entropy as the basis of clustering [2, 14] mainly focused on categorical datasets. In many cases, the task of object detection is to localize a large number of objects belonging to a wide range of distinct categories. Therefore, developing a clustering module which makes use of pixel-wise information instead of their distance, may be of significant importance for improving existing clustering methods.

Therefore, in this work, we propose the ENtropy-based Attention Clustering for detection Transformers (ENACT), which operates as follows. Firstly, the probability density function of the Key input is estimated using a linear layer and a softmax function. Subsequently, the self-information of each pixel is calculated using the estimated distribution and the final grouping is done on the basis of the curvature of the information signal. Specifically, the regions with same sign of second derivative, in consecutive sign change regions, are grouped together. The clustered Keys and Values are then passed on to the self-attention layer of the encoder.

The main contributions of this work can be summarized as follows:

- We propose and provide ENACT, a module which clusters the Keys and Values, before being fed into the encoder of a detection transformer, on the basis of the

self-information of each Key pixel using a learned distribution.

- The developed module can serve as a *plug-in to any detection transformer* architecture as long as its encoder includes the passing of the Queries, Keys and Values into a multi-head self attention module (MHSA). Additionally, the clustering is based on the Key pixels' self-information similarity. Therefore, *the number of clusters is not a hyper-parameter* and instead, its computation is data-driven.
- We plug ENACT to three Detection Transformers [4, 22, 30] and we show that we obtain similar precision, while saving about 20-40% GPU RAM, and 5-15% training time depending on the detector.

2. Related Work

2.1. Transformer models

Transformer networks were initially developed to deal with sequence translation problems (i.e. text-to-text translation etc.). Vaswani *et al.* [26] who introduced them, used an encoder-decoder architecture where the input passes through a self-attention module in order to learn the connections between queries and keys. Subsequently, transformers were deployed to solve vision problems by combining the encoder-decoder structure with a convolutional backbone for the extraction of feature maps. Works like the Vision Transformer (ViT), Swin-Transformer and Pyramid Vision Transformer [6, 19, 29] are prime examples of this approach. The need to apply transformer models in object detection tasks was soon realized because detectors such as Fast R-CNN [11], Faster R-CNN [24], YOLO [23], SSD [18] and RetinaNet [15], despite achieving benchmark detection performances on challenging datasets need a number of manually crafted components like Region Proposal Networks or Non Maximum Suppression. For the resolution of the latter issue, Carion *et al.* [4] proposed the Detection Transformer (DETR), which implements a bipartite matching loss that unilaterally connects a prediction to a ground truth object, in addition to a transformer-based encoder-decoder structure. That way the need for manual non-maximum suppression and anchor generation was removed while outperforming, at the same time, existing object detectors in terms of precision.

Nonetheless, one predominant problem that remained, was the large complexity and training time required for convergence. To that end, Zhu *et al.* [35] proposed the Deformable DETR algorithm, where the attention of each pixel is focused on a predetermined number of points, with learnable attention weights and point locations. This significantly reduced training time, but the number of attention points was a hyperparameter which is dataset-

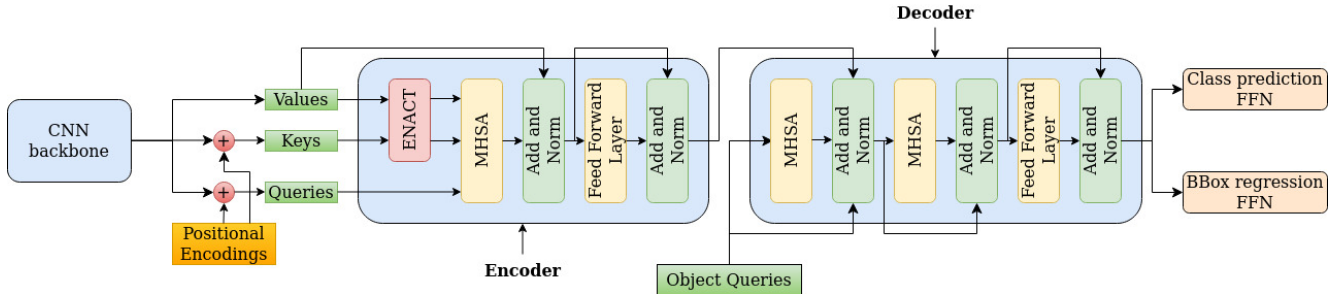


Figure 1. Visualization of a detection transformer with the addition of the ENACT module. The feature maps obtained from the CNN backbone, are the Queries, Keys and Values, with the former two being supplemented with positional encodings. All three pass through the encoder, with the Keys and Values being clustered by the ENACT module. Subsequently, the Queries, as well as the clustered Keys and Values pass through the multi-head self-attention module (MHSA), making it faster in computation and cheaper in memory usage.

specific. It also included inputs from more than one convolutional layers from the backbone, so the attention module of this method is called Multi Scale Deformable Attention (MSDA). Another method that was proposed by Katharopoulos *et al.* [13] reduced the complexity of the attention calculation from quadratic to linear by making use of the associativity property of matrix products. Wang *et al.* [30] proposed the Anchor DETR, which aimed at resolving the miscorrelation between positionally encoded object queries and image regions by matching the object queries with anchors. Another work which focused on resolving the slow convergence of detection transformers, was proposed by Yao *et al.* called Efficient DETR [31], which shown that by using the output of the detection head as prior initialization of the decoder input, there is no need for many decoder layers and the associated computations. Meng *et al.* proposed the Conditional DETR [22], which also resolves the slow training time, by learning spatial queries for the decoder cross attention, making it focus on the bounding box extremes and regions within the box. More recent works that achieve state-of-the-art detection performances in benchmark object detection tasks (i.e., COCO detection [16]) are the DINO [33] and the Co-DETR [36] models. The former, uses the output of the encoder as a prior for learnable queries for the decoder, and the latter implements a hybrid assignment scheme using auxiliary heads in the decoder to reduce the impact of the large number of negative examples in the object queries. It should be noted that neither of these two last models consists of an MHSA module in the encoder, but instead use the MSDA implemented in the Deformable DETR [35].

2.2. Clustering transformers

Another way to reduce the complexity and training time of transformers for object detection is by reducing the size of the attention inputs. The most straightforward approach to achieve that is by implementing clustering methods. There is a wide range of clustering algorithms avail-

able that are either centroid based (e.g. k-means [9, 20], mean-shift [10]) or density based (e.g. DBSCAN [7], OPTICS [1]), which are possible candidates for the reduction of the attention input. Vyas *et al.* [27] used k-means to group queries into clusters, and then computed the attention between the query centroids and the best matching key-pair to each of the centroids. Zheng *et al.* [34] proposed the Adaptive Clustering Transformer (ACT) which clusters the queries into prototypes using locality sensitive hashing to group queries with small Euclidean distance. Zeng *et al.* [32] proposed the TCFormer which focused on the progressive aggregation of initially small clusters (i.e., the pixels themselves) to larger ones that capture regions with similar semantic information.

2.3. Entropy-based clustering

Although the idea of using the entropy of the input as a way to group pixels together has not been used in detection transformers, it has been used in works that focused on the clustering of categorical inputs. Barbara *et al.* [2] proposed the COOLCAT model which clusters data streams of categorical data incrementally using the cluster entropy. Li *et al.* [14] also focused on clustering categorical data using entropy, starting by placing all points in one cluster and iteratively replacing the cluster attributions of random data points, if the new configurations led to entropy decrease. Using entropy in a transformer-like structure was done by Liu *et al.* [17] but instead of clustering, it was used for learned image compression. The presented experiments showed that the performance of the compression surpassed previous methods.

3. Method

3.1. Overview

In this work we propose the ENACT module which provides a data-driven way to cluster the input of the self-attention module of a transformer encoder. The clustering

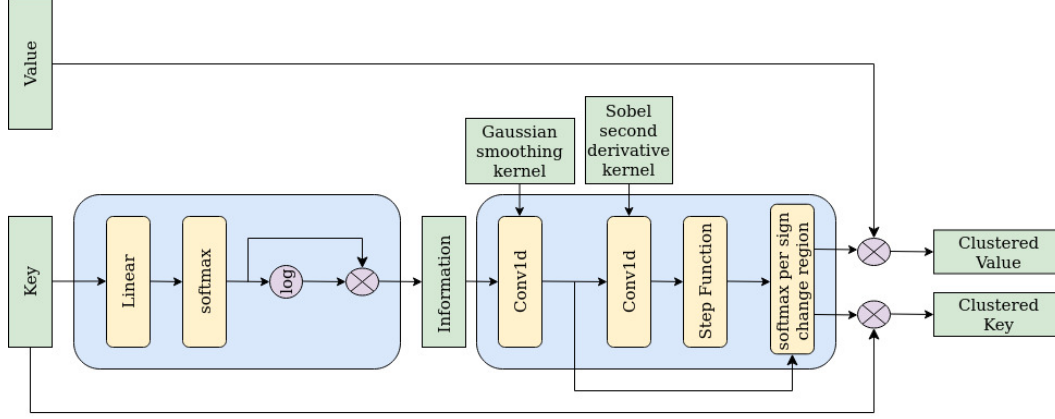


Figure 2. Overview of the ENACT module. The key passes through the network responsible for the calculation of the information and subsequently the information is smoothed by a Gaussian kernel. Then, the regions where the information is a convex or concave function are identified by the second derivative and a softmax function is applied to the information values of each separate region of same sign in second derivative. The clustering is done by summing the weighted information values multiplied by the respective feature vectors of the values and keys, per region.

is conducted on the basis of the entropy of the input, and specifically, on the self-information yielded by each pixel of the feature map. Due to the fact that there is no requirement for prior knowledge concerning the distribution of the features, there are no hyperparameters that have to do with the information calculation or with the clustering implementation, namely there is *no pre-determination of the number of clusters*.

The ENACT module serves as a plug-in component to the standard detection transformer architecture (see Figure 1), which renders it applicable to any such model. Specifically, the encoder should consist of the following parts: MHSA, normalization layer, Feed Forward Network (FFN), normalization layer. Furthermore, it reduces the size of the input, which has an effect on both the GPU memory required for training, as well as the training and inference time.

It is important to note that ENACT can be employed by transformer models that include an MHSA module in the encoder but not MSDA. This is why it cannot be plugged into more modern models like DINO [33] or Co-DETR [36]. The reason for this is that MSDA does not compute attention using the dot-product function between Queries and Keys (see Equations 1, 2). Instead, only the Queries pass through two linear layers that compute attention weights and directions to a predetermined or learned number of “reference” pixels, and the respective feature vector from the Values is multiplied with the respective computed weights. As a result, clustering the input would decrease the size of the output of each consecutive encoder layer which is very likely to lead to considerable precision decrease.

In the original detection transformers, Queries (Q), Keys

(K) and Values (V), have the same dimensions, namely $Q, K, V \in \mathbb{R}^{N \times HW \times d}$, where N is the batch size, HW the total number of pixels in the feature map, and d the dimensions of the feature vector. This means that the resulting attention weight matrix $A \in \mathbb{R}^{N \times HW \times HW}$ is quadratic with respect to the spatial dimensions. In the ENACT model we cluster the Keys and the Values before passing them to the attention module, and the resulting $K_{cl}, V_{cl} \in \mathbb{R}^{N \times H'W' \times d}$ where $H'W' < HW$. Therefore, the clustered attention weight matrix $A_{cl} \in \mathbb{R}^{N \times HW \times H'W'}$ is much less consuming in memory space. Additionally, since the Values are also clustered, the matrix multiplication between attention weights and values, which is done in order to compute the attention map (\mathcal{A}), will be done along the axis of the reduced spatial dimensions. This will make the computation of the clustered attention map (\mathcal{A}_{cl}) faster. To clarify this, in Eq. 1 and Eq. 2 we show how the attention weights and attention map, are calculated in the attention module.

$$A = \text{softmax} \left(\frac{Q \cdot K^T}{\sqrt{d}} \right), A_{cl} = \text{softmax} \left(\frac{Q \cdot K_{cl}^T}{\sqrt{d}} \right). \quad (1)$$

$$\mathcal{A} = A \cdot V, \mathcal{A}_{cl} = A_{cl} \cdot V_{cl}. \quad (2)$$

The Queries are left un-clustered because we want the final attention map to maintain its size after each encoder layer, for the reason described previously. In detection transformers, the Queries, Keys and Values are the same, with the exception that Queries and Keys are supplemented with positional encodings, that add information about the location of each pixel.

The ENACT module (see Figure 2), consists of two main

components. The first is responsible for the computation of the self-information of the input pixels, and the second implements the clustering based on the regions where there is observable information gain or loss. Since, we cluster the Keys and Values, we have to choose whose entropy will be the one on which the clustering will be based on. The input chosen for that are the Keys because they are supplemented with positional encodings, and we consider that the information that corresponds to the location of each feature vector is useful to the calculation of the entropy. This is because pixels with information regarding an object in an image, are likely to also be close to each other and the positional information is indicative of this proximity. Another important note is that we plug the ENACT model only inside the encoder of the transformer. This is because the input of the decoder is originally Gaussian noise and the computation of the pixels' self-information will not have any significant value. Another reason is that the decoder input is a trainable parameter, and clustering the input originating from Gaussian noise may be detrimental for the object query training.

3.2. Information calculation

The clustering is done on the basis of the self-information each pixel has, as shown in Eq. 3, where x is the feature vector of a pixel, and $p(x)$ is the probability density function of the vector distribution. We can see that the computed quantity is the one inside the sum of the Shannon entropy.

$$\mathcal{H}(x) = -p(x)\log(p(x)). \quad (3)$$

The p.d.f. is learnable since it is calculated by passing the input through a linear layer that maps it from the feature dimensions to 1 and the result is passed through a softmax function, making the sum of the probabilities across all pixels to be equal to one. This is shown in Eq. 4, where W is the weight matrix initialized from a Xavier uniform distribution and has size $(1 \times d)$, and b is the bias with size equal to 1.

$$p(x) = \text{softmax}(x \cdot W^T + b). \quad (4)$$

Therefore, the final output of the information module is a signal with shape (batch size $\times HW$) where HW is the total number of pixels in the feature map.

3.3. Clustering process

Having obtained the information from the first module, we use it to cluster the attention Keys and Values. To do that we firstly convolve the information with a 1D Gaussian kernel. This is done because in the resulting information there may be cases with consecutive sharp edges in the signal due to noise, and in order to alleviate this problem, it is required to smooth the signal. The kernel itself is shown in Eq. 5,

where the x is a 1D vector of integers that range from -3σ to 3σ :

$$G(x) = \frac{1}{\sqrt{2\pi\sigma}} \exp(x^2/2\sigma^2), x \in \mathbb{Z} : x \in [-3\sigma, 3\sigma] \quad (5)$$

The value of the standard deviation σ is an experimentally determined hyperparameter.

After the smoothing is completed, we compute the regions where the signal is concave and convex. To do so, we first estimate its second derivative using the Sobel kernel in Eq. 6.

$$\text{Sobel}''(x) = [-1, 2, -1]. \quad (6)$$

The reason we do this is because we consider the regions where the local information gain or loss is apparent as the most suitable for clustering, since, for example, a pixel with an information local maximum/minimum and its surroundings could be clustered as one entity.

Subsequently, we pass the second derivative of the information to a step function which attributes 1 to the convex parts of the information curve, and 0 to the concave ones. Concave regions signify information gain, and convex ones signify loss.

At that point, we take the smoothed entropy and we run a softmax function on each separate region whose indices correspond to regions of the same sign in the output of the step function. For example, assume that at one point the output of the step function is $[\dots, 1, 1, 1, 0, 1, 1, 1, \dots]$ and the indices are $[\dots, i, i+1, \dots, i+8, \dots]$. In the respective indices of the entropy the softmax function will be run on three separate regions, which are from i to $i+2$, $i+3$ to $i+4$ and $i+5$ to $i+8$. The exact computation is shown in Eq. 7, where \mathcal{H}_j is the self-information of pixel j .

$$\begin{aligned} \mathcal{H}_j &= \frac{\exp(\mathcal{H}_j)}{\sum_{k=i}^{i+2} \exp(\mathcal{H}_k)} \text{ if } j \in [i, i+2] \\ \mathcal{H}_j &= \frac{\exp(\mathcal{H}_j)}{\sum_{k=i+3}^{i+4} \exp(\mathcal{H}_k)} \text{ if } j \in [i+3, i+4] \\ \mathcal{H}_j &= \frac{\exp(\mathcal{H}_j)}{\sum_{k=i+5}^{i+8} \exp(\mathcal{H}_k)} \text{ if } j \in [i+5, i+8] \end{aligned} \quad (7)$$

The final step is to multiply the resulting weighted entropies with the respective feature vectors from the Keys and Values, and sum the results per cluster.

4. Experiments

4.1. Dataset

We evaluate our model on the MS COCO 2017 dataset [16], which is a benchmark dataset for object detection. The images include objects in complex environments, making the task of detection more realistic and applicable to real-life scenarios. In total, the dataset consists of 91 classes which are frequently occurring objects in everyday scenes (e.g. car, tv, chair etc.). Relative to other object detection datasets (e.g. PASCAL VOC [8]), MS COCO has, on average, more instances per image, and also a bigger diversity of categories per image. The 2017 version of the dataset is split into train, validation and test sets, which consist of 118,000, 5,000 and 41,000 images, respectively. Annotations are provided only for the former two sets, and they include information regarding the image id, the bounding box of the included objects, as well as their class. Segmentation masks are also provided for object segmentation tasks. Since annotations are not available for the test set, we use only the training part of the dataset for training, and we evaluate the overall performance on the validation set.

4.2. Experimental setting

As it was mentioned in Section 3.1, the inputs of the encoder are the queries, keys and values. Out of these, the latter two pass through the ENACT module for dimensional consistency reasons, and the entropy is computed only from the Keys. The parameters are initialized from a Xavier uniform distribution, meaning that the weights are initialized from a uniform distribution, whose edges are inversely proportional to the square root of the input and output dimensions of the layer, and the biases are initially zero. The output of the linear layer responsible for computing the probability distribution of the input is added with a very small value ($1e-8$) in order to avoid errors due to zeros in the log during the calculation of the entropy.

We evaluate ENACT’s performance by applying it to three detection transformers. These are the Detection Transformer (DETR) [4], the Conditional DETR [22] and the Anchor DETR [30]. For DETR and Anchor DETR, we use the ResNet-50 [12] backbone, whereas for Conditional DETR, we use ResNet-101. Both are pretrained on ImageNet [5]. Additionally, for all three variants, we use the AdamW optimizer [21]. The learning rate is set to $5e-5$ for all three transformer models, and all three follow a learning rate drop schedule which reduces its value to a tenth of the original. DETR drops the learning rate after 200 epochs, while Anchor and Conditional DETR after 40 epochs. The weight decay is set to $1e-4$. Anchor DETR and Conditional DETR are trained for 50 epochs in total, and DETR is trained for 300 epochs. The batch size is set to 4 for the Anchor-DETR and 8 for the other two transformers. For our experiments,

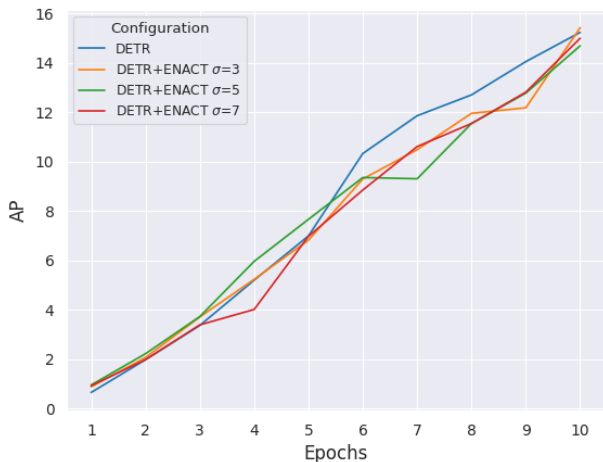


Figure 3. AP per epoch for the first 10 epochs of the DETR training with the ENACT module for $\sigma = 3, 5, 7$. For comparison, we also provide the results of training the plain DETR model during the same 10 epochs.

we used an NVIDIA RTX A6000 GPU with 49GB RAM.

Regarding the module’s parameters, we only have to determine the standard deviation σ of the Gaussian smoothing kernel, which is convolved with the entropy. Depending on the performance gain with respect to several factors which will be described later, we decided the respective optimal value of σ for each of the detection transformers used. For DETR and Conditional DETR, we set $\sigma = 3$, and for Anchor DETR we set $\sigma = 5$ (see Section 4.4). Regarding Anchor DETR, the attention mechanism used is not the original multi-head self-attention, but the Row-Column Decoupled Attention (RCDA). This means that the attention is computed per row and column, and the result is merged to produce the final outcome. This poses a problem for ENACT, since we have to decide to compute the entropy based on either the Key rows or columns, or find a way to merge the entropy computed from both. It turns out that we can do the former, because the regions of information gain and loss are almost identical whether we use the Key rows or columns (see Section 4.4).

4.3. Evaluation metrics

To evaluate the proposed ENACT module, we measure its training time and its memory usage. Another metric which is important due to its value in real life applications is inference time, i.e., the time required for predictions. Gains in the aforementioned metrics come at the cost of data size, which inevitably leads to losses in prediction precision. Precision itself is computed using the average precision metric (AP), which is the most inclusive precision metric in terms of size and class factors. Additional metrics are the AP for

Model	GPU RAM (GB)	GPU Gain (%)	training time (s/image)	Inference time (s/image)
DETR [4]	36.5	-	0.0541	0.0482
DETR + ENACT	23.5	35.6	0.0488	0.0472
Anchor DETR [30]	29.7	-	0.0999	0.0712
Anchor DETR + ENACT	17.7	40.4	0.0845	0.0608
Conditional DETR [22]	46.6	-	0.0826	0.0637
Conditional DETR + ENACT	36.7	20.4	0.0779	0.0605

Table 1. Comparison of GPU RAM consumption, training and inference time, for three detection transformers, with and without the plugging of the ENACT module. We also show the GPU memory percentage gain when using ENACT. The time is computed in seconds per image, but Anchor-DETR is trained and tested with batch size 4, while the other two transformers with batch size 8.

Model	Epochs	AP	AP ₅₀	AP ₇₅	AP _s	AP _m	AP _l
RetinaNet [23]	36	38.7	58.0	41.5	23.3	42.3	50.3
Faster RCNN [24]	36	40.2	61.0	43.8	24.2	43.5	52.0
RSDNet [†] [28]	12	40.3	60.1	43.0	22.1	43.5	51.5
FCOS [25]	36	41.4	60.1	44.9	25.6	44.9	53.1
Cascade R-CNN [†] [3]	12	42.7	61.6	46.6	23.8	46.2	57.4
DETR-C5 [4]	300	40.6	61.6	-	19.9	44.3	60.2
DETR-C5 + ENACT (ours)	300	39.0	59.1	41.3	18.3	42.2	57.0
Anchor DETR-DC5 [30]	50	44.3	64.9	47.7	25.1	48.1	61.1
Anchor DETR-DC5 + ENACT (ours)	50	42.9	63.5	45.9	25.0	46.8	58.5
Conditional DETR-C5 [†] [22]	50	42.8	63.7	46.0	21.7	46.6	60.9
Conditional DETR-C5 + ENACT [†] (ours)	50	41.5	62.2	44.3	21.3	45.5	59.3

Table 2. Detection performance results in terms of precision, as well as number of training epochs, for different object detectors, on the COCO 2017 test-dev. Red and blue colors correspond to the best and second best performance, respectively. DC5 and C5 denote whether the last convolutional layer in the DETR based models is dilated or not, respectively. All models share the ResNet-50 backbone, unless denoted by [†] which means they were trained using ResNet-101 backbone. (AP₇₅ not available in DETR 300 epoch schedule).

predictions where the Intersection over Union (IoU) overlap exceeds 50% and 75% (AP₅₀, AP₇₅) and the AP for small, medium and large objects (AP_s, AP_m, AP_l).

4.4. Ablation studies

With respect to hyperparameter tuning in the ENACT module, we only have to determine the standard deviation of the Gaussian smoothing kernel as mentioned in Section 4.2. The optimal decision varies per detector used, and depends on the value that leads to maximum precision and maximum gain in memory and training time. In Figure 3, we show the training curves of the DETR model with the ENACT module attached during the first 10 epochs of training, for $\sigma = 3, 5, 7$. We observe that for $\sigma = 3$ we get the maximum AP at epoch 10, even higher than the one of the plain DETR at the same epoch. A similar approach is followed for determining the optimal σ for Anchor DETR and Conditional DETR. In the case of Anchor DETR, at epoch 2, $\sigma = 3$ yielded AP 15.3, whereas $\sigma = 5$ yielded AP 16.4 with a significant reduction on GPU memory of $\sim 50\%$. Therefore, for Anchor DETR, we set $\sigma = 5$. As mentioned previously, Anchor DETR implements row-column decoupling and we only use the Key rows for the computation

of the entropy, which as we said, leads to almost identical regions. Specifically, we observe that the cluster regions resulting from using the Key rows and then the Key columns for the computation of the entropy are similar by 95% on average. Finally, regarding Conditional DETR, at epoch 2, $\sigma = 3$ yielded AP 12.36, whereas $\sigma = 5$ yielded AP 12.34, and the GPU memory usage was similar. Therefore, we kept $\sigma = 3$ for the remainder of the training.

4.5. Results

4.5.1 Quantitative results

We present the overall performance of the ENACT module, when plugged into the three mentioned detection transformers. Starting with the GPU requirements, in Table 1 we show the RAM consumption of the GPU when using the three detection transformer variants, and when plugging in the ENACT module to each of them. The results are those obtained during training so that both forward pass inputs and backward pass gradients are included. We can observe that by supplementing each of the detection transformers with the ENACT module, we consistently reduce the GPU consumption by a margin which ranges from 20% to 40%.

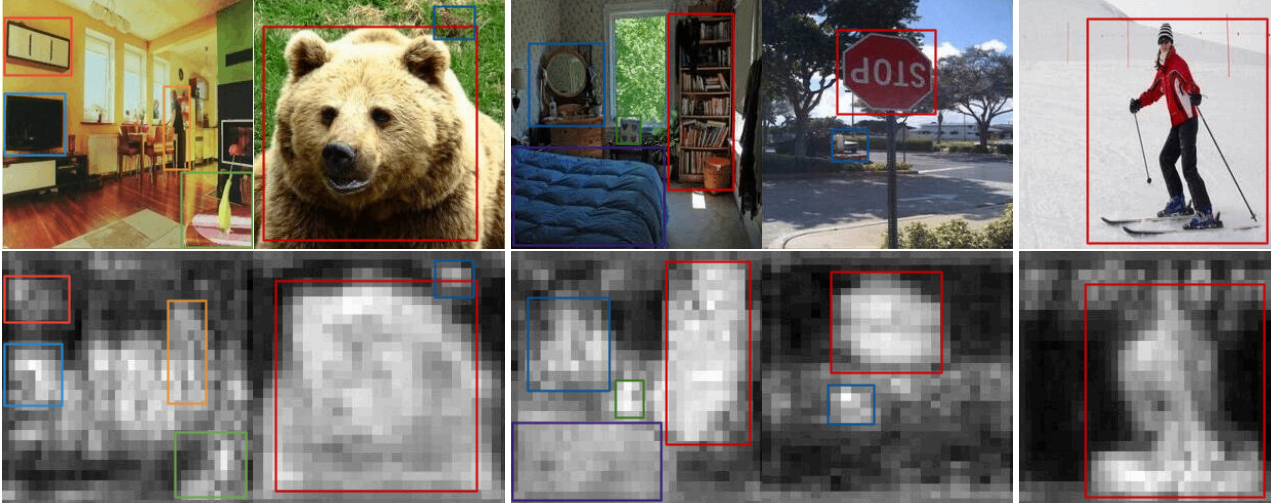


Figure 4. A selection of images from the COCO dataset (above), with the respective output of the self-information module prior to the Gaussian smoothing (below). Bright pixels in the bottom images, correspond to regions that yield higher information. We use same-color bounding boxes, to show corresponding objects between images and information maps.

This constitutes a significant reduction in computational resources, which can extend the deployment of such transformer models by smaller GPUs.

Subsequently, we evaluate the performance of the ENACT module with regard to its capacity of reducing the total training time required by the model upon which it is applied. In the same manner as for the GPU memory usage, we use the models with and without ENACT, and we compare the time per image required in both cases. The results are also shown in Table 1, where we show the time per image required in both cases for the same three detection transformers. It can be verified that the training time required is reduced by 5.6% in the Conditional DETR model, 9.8% in the DETR model and 15.4% in the Anchor DETR model. Therefore, the reduction of the Keys and Values sizes used in the self-attention function, indeed reduces the time required for the dot product operations. Moreover, it is observed that the gain obtained in terms of inference time ranges from 2% in the DETR, to 14% in the Anchor DETR.

Finally, we evaluate the performance obtained by the plugging of the ENACT module in terms of precision and present the results in Table 2. We observe that the obtained APs are very close to those of the original transformer models, with the reductions being 1.3% for the Conditional DETR, 1.6% for the DETR and 1.4% for the Anchor DETR. Those are fairly slight drops and the resulting precisions still surpass several existing object detectors in the same dataset.

4.5.2 Qualitative results

One of the important aspects of this work that has to be verified is the extent to which the idea of computing the self-

information of each pixel is valid. Besides verifying experimentally that ENACT drops the needed computational resources without affecting considerably the detection precision, it is also important to visualize the output obtained from the first part of the ENACT module, which is responsible for computing the self-information of the feature map pixels. Some relevant, indicative results are shown in Figure 4. Specifically, we use the ENACT module plugged in the Conditional DETR and we pass the images through the trained model of the final epoch. We observe that for the most part, the visualized information map is brighter in regions where objects are located, and dimmer in the background. Considering the fact that the probability density function is learnable, we can see that the final trained model, in the part responsible for computing the information, correctly learned that the most informative pixels are the ones that correspond to objects of interest.

5. Summary

We presented ENACT, a clustering module for MHSA-based detection transformers, which compresses the encoder input on the basis of its entropy. We showed that the pixel-wise self-information is indeed correlated to the important objects in the image, thereby rendering it as a valid metric for clustering. We trained three detection transformers using ENACT, and we show that we can obtain approximately 30% decrease in GPU memory, 10% decrease in training and inference time, while losing only 1.5% in average precision. This makes ENACT a reliable plug-in for this type of transformer models, which can reduce significantly their computational requirements without compromising considerably their object detection capabilities.

References

- [1] Mihael Ankerst, Markus M Breunig, Hans-Peter Kriegel, and Jörg Sander. Optics: Ordering points to identify the clustering structure. *ACM Sigmod record*, 28(2):49–60, 1999. 3
- [2] Daniel Barbará, Yi Li, and Julia Couto. Coolcat: an entropy-based algorithm for categorical clustering. In *Proceedings of the eleventh international conference on Information and knowledge management*, pages 582–589, 2002. 2, 3
- [3] Zhaowei Cai and Nuno Vasconcelos. Cascade r-cnn: Delving into high quality object detection. In *Proceedings of the IEEE conference on computer vision and pattern recognition*, pages 6154–6162, 2018. 7
- [4] Nicolas Carion, Francisco Massa, Gabriel Synnaeve, Nicolas Usunier, Alexander Kirillov, and Sergey Zagoruyko. End-to-end object detection with transformers. In Andrea Vedaldi, Horst Bischof, Thomas Brox, and Jan-Michael Frahm, editors, *Computer Vision – ECCV 2020*, pages 213–229, Cham, 2020. Springer International Publishing. 1, 2, 6, 7
- [5] Jia Deng, Wei Dong, Richard Socher, Li-Jia Li, Kai Li, and Li Fei-Fei. Imagenet: A large-scale hierarchical image database. In *2009 IEEE Conference on Computer Vision and Pattern Recognition*, pages 248–255, 2009. 6
- [6] Alexey Dosovitskiy, Lucas Beyer, Alexander Kolesnikov, Dirk Weissenborn, Xiaohua Zhai, Thomas Unterthiner, Mostafa Dehghani, Matthias Minderer, Georg Heigold, Sylvain Gelly, Jakob Uszkoreit, and Neil Houlsby. An image is worth 16x16 words: Transformers for image recognition at scale. In *International Conference on Learning Representations*, 2021. 2
- [7] Martin Ester, Hans-Peter Kriegel, Jörg Sander, Xiaowei Xu, et al. A density-based algorithm for discovering clusters in large spatial databases with noise. In *kdd*, volume 96, pages 226–231, 1996. 3
- [8] Mark Everingham, Luc Van Gool, Christopher KI Williams, John Winn, and Andrew Zisserman. The pascal visual object classes (voc) challenge. *International journal of computer vision*, 88:303–338, 2010. 6
- [9] Edward W Forgy. Cluster analysis of multivariate data: efficiency versus interpretability of classifications. *biometrics*, 21:768–769, 1965. 3
- [10] Keinosuke Fukunaga and Larry Hostetler. The estimation of the gradient of a density function, with applications in pattern recognition. *IEEE Transactions on information theory*, 21(1):32–40, 1975. 3
- [11] Ross Girshick. Fast r-cnn. In *Proceedings of the IEEE international conference on computer vision*, pages 1440–1448, 2015. 1, 2
- [12] Kaiming He, Xiangyu Zhang, Shaoqing Ren, and Jian Sun. Deep residual learning for image recognition. In *2016 IEEE Conference on Computer Vision and Pattern Recognition (CVPR)*, pages 770–778, 2016. 6
- [13] Angelos Katharopoulos, Apoorv Vyas, Nikolaos Pappas, and François Fleuret. Transformers are rnns: Fast autoregressive transformers with linear attention. In *International conference on machine learning*, pages 5156–5165. PMLR, 2020. 3
- [14] Tao Li, Sheng Ma, and Mitsunori Ogihara. Entropy-based criterion in categorical clustering. In *Proceedings of the twenty-first international conference on Machine learning*, page 68, 2004. 2, 3
- [15] Tsung-Yi Lin, Priya Goyal, Ross Girshick, Kaiming He, and Piotr Dollár. Focal loss for dense object detection. In *Proceedings of the IEEE international conference on computer vision*, 2017. 1, 2
- [16] Tsung-Yi Lin, Michael Maire, Serge Belongie, James Hays, Pietro Perona, Deva Ramanan, Piotr Dollár, and C Lawrence Zitnick. Microsoft coco: Common objects in context. In *Computer Vision–ECCV 2014: 13th European Conference, Zurich, Switzerland, September 6–12, 2014, Proceedings, Part V 13*, pages 740–755. Springer, 2014. 3, 6
- [17] Jinming Liu, Heming Sun, and Jiro Katto. Learned image compression with mixed transformer-cnn architectures. In *Proceedings of the IEEE/CVF conference on computer vision and pattern recognition*, pages 14388–14397, 2023. 3
- [18] Wei Liu, Dragomir Anguelov, Dumitru Erhan, Christian Szegedy, Scott Reed, Cheng-Yang Fu, and Alexander C. Berg. Ssd: Single shot multibox detector. In Bastian Leibe, Jiri Matas, Nicu Sebe, and Max Welling, editors, *Computer Vision – ECCV 2016*, pages 21–37, Cham, 2016. Springer International Publishing. 1, 2
- [19] Ze Liu, Yutong Lin, Yue Cao, Han Hu, Yixuan Wei, Zheng Zhang, Stephen Lin, and Baining Guo. Swin transformer: Hierarchical vision transformer using shifted windows. In *Proceedings of the IEEE/CVF international conference on computer vision*, pages 10012–10022, 2021. 2
- [20] Stuart Lloyd. Least squares quantization in pcm. *IEEE transactions on information theory*, 28(2):129–137, 1982. 3
- [21] Ilya Loshchilov and Frank Hutter. Decoupled weight decay regularization. In *International Conference on Learning Representations*, 2019. 6
- [22] Depu Meng, Xiaokang Chen, Zejia Fan, Gang Zeng, Houqiang Li, Yuhui Yuan, Lei Sun, and Jingdong Wang. Conditional detr for fast training convergence. In *Proceedings of the IEEE/CVF international conference on computer vision*, pages 3651–3660, 2021. 2, 3, 6, 7
- [23] J. Redmon, S. Divvala, R. Girshick, and A. Farhadi. You only look once: Unified, real-time object detection. In *2016 IEEE Conference on Computer Vision and Pattern Recognition (CVPR)*, pages 779–788, Los Alamitos, CA, USA, jun 2016. IEEE Computer Society. 1, 2, 7
- [24] Shaoqing Ren, Kaiming He, Ross Girshick, and Jian Sun. Faster r-cnn: Towards real-time object detection with region proposal networks. In C. Cortes, N. Lawrence, D. Lee, M. Sugiyama, and R. Garnett, editors, *Advances in Neural Information Processing Systems*, volume 28. Curran Associates, Inc., 2015. 1, 2, 7
- [25] Zhi Tian, Chunhua Shen, Hao Chen, and Tong He. Fcos: Fully convolutional one-stage object detection. In *Proceedings of the IEEE/CVF International Conference on Computer Vision (ICCV)*, October 2019. 7
- [26] Ashish Vaswani, Noam Shazeer, Niki Parmar, Jakob Uszkoreit, Llion Jones, Aidan N Gomez, Łukasz Kaiser, and Illia Polosukhin. Attention is all you need. *Advances in neural information processing systems*, 30, 2017. 1, 2

- [27] Apoorv Vyas, Angelos Katharopoulos, and François Fleuret. Fast transformers with clustered attention. *Advances in Neural Information Processing Systems*, 33:21665–21674, 2020. [1](#), [3](#)
- [28] Shaoru Wang, Yongchao Gong, Junliang Xing, Lichao Huang, Chang Huang, and Weiming Hu. Rdsnet: A new deep architecture for reciprocal object detection and instance segmentation. In *Proceedings of the AAAI conference on artificial intelligence*, volume 34, pages 12208–12215, 2020. [7](#)
- [29] Wenhai Wang, Enze Xie, Xiang Li, Deng-Ping Fan, Kaitao Song, Ding Liang, Tong Lu, Ping Luo, and Ling Shao. Pyramid vision transformer: A versatile backbone for dense prediction without convolutions. In *Proceedings of the IEEE/CVF international conference on computer vision*, pages 568–578, 2021. [2](#)
- [30] Yingming Wang, Xiangyu Zhang, Tong Yang, and Jian Sun. Anchor detr: Query design for transformer-based detector. In *Proceedings of the AAAI conference on artificial intelligence*, volume 36, pages 2567–2575, 2022. [2](#), [3](#), [6](#), [7](#)
- [31] Zhuyu Yao, Jiangbo Ai, Boxun Li, and Chi Zhang. Efficient detr: improving end-to-end object detector with dense prior. *arXiv preprint arXiv:2104.01318*, 2021. [3](#)
- [32] Wang Zeng, Sheng Jin, Wentao Liu, Chen Qian, Ping Luo, Wanli Ouyang, and Xiaogang Wang. Not all tokens are equal: Human-centric visual analysis via token clustering transformer. In *Proceedings of the IEEE/CVF Conference on Computer Vision and Pattern Recognition*, pages 11101–11111, 2022. [1](#), [3](#)
- [33] Hao Zhang, Feng Li, Shilong Liu, Lei Zhang, Hang Su, Jun Zhu, Lionel Ni, and Heung-Yeung Shum. DINO: DETR with improved denoising anchor boxes for end-to-end object detection. In *The Eleventh International Conference on Learning Representations*, 2023. [3](#), [4](#)
- [34] Minghang Zheng, Peng Gao, Renrui Zhang, Kunchang Li, Hongsheng Li, and Hao Dong. End-to-end object detection with adaptive clustering transformer. In *32nd British Machine Vision Conference 2021, BMVC 2021, Online, November 22-25, 2021*, page 226. BMVA Press, 2021. [1](#), [3](#)
- [35] Xizhou Zhu, Weijie Su, Lewei Lu, Bin Li, Xiaogang Wang, and Jifeng Dai. Deformable {detr}: Deformable transformers for end-to-end object detection. In *International Conference on Learning Representations*, 2021. [1](#), [2](#), [3](#)
- [36] Zhuofan Zong, Guanglu Song, and Yu Liu. Detr with collaborative hybrid assignments training. In *Proceedings of the IEEE/CVF international conference on computer vision*, pages 6748–6758, 2023. [3](#), [4](#)